Cerebral microbleeds: a guide to detection and interpretation

Steven M Greenberg, Meike W Vernooij, Charlotte Cordonnier, Anand Viswanathan, Rustam Al-Shahi Salman, Steven Warach, Lenore J Launer, Mark A Van Buchem, Monique M B Breteler; for the Microbleed Study Group

Cerebral microbleeds (CMBs) are increasingly recognised neuroimaging findings in individuals with cerebrovascular disease and dementia, and in normal ageing. There has been substantial progress in the understanding of CMBs in recent years, particularly in the development of newer MRI methods for the detection of CMBs and the application of these techniques to population-based samples of elderly people. In this Review, we focus on these recent developments and their effects on two main questions: how CMBs are detected, and how CMBs should be interpreted. The number of CMBs detected depends on MRI characteristics, such as pulse sequence, sequence parameters, spatial resolution, magnetic field strength, and image post-processing, emphasising the importance of taking into account MRI technique in the interpretation of study results. Recent investigations with sensitive MRI techniques have indicated a high prevalence of CMBs in community-dwelling elderly people. We propose a procedural guide for identification of CMBs and suggest possible future approaches for elucidating the role of these common lesions as markers for, and contributors to, small-vessel brain disease.

Lancet Neurol 2009; 8: 165–74

Department of Neurology, Massachusetts General Hospital, Harvard Medical School, Boston, USA (S M Greenberg MD, A Viswanathan MD); **Department of Radiology** (M W Vernooij MD) **and Department of Epidemiology, Erasmus MC University Medical Center, Rotterdam, Netherlands** (M W Vernooij, M M B Breteler MD); **Department of Neurology (Stroke Department), Lille University Hospital, Lille, France** (C Cordonnier MD); **Division of Clinical Neurosciences, University of Edinburgh, Western General Hospital, Edinburgh, UK** (R Al-Shahi Salman FRCP); **Stroke Branch, National Institute of Neurological Disorders and Stroke, Bethesda, USA** (S Warach MD); **Laboratory of Epidemiology, Biometry, and Demography, National Institute on Aging, Bethesda, USA** (L J Launer PhD); **and Department of Radiology, Leiden University Medical Center, Leiden, Netherlands** (M A Van Buchem MD)

Correspondence to:
Steven M Greenberg, Department of Neurology, Massachusetts General Hospital, 175 Cambridge Street, Suite 300, Boston, MA 02114, USA
sgreenberg@partners.org

Introduction

Small foci of chronic blood products in normal (or near normal) brain tissue, known as cerebral microbleeds (CMBs), have become increasingly recognised with the widespread use of MRI techniques that are sensitive to iron deposits.[1,2] Advances in software and hardware have led to substantial increases in the sensitivity of MRI to CMBs and improvements in the criteria for their identification. Another area of recent progress has been the use of sensitive MRI in community-dwelling elderly people, in whom the prevalence of CMBs detected is as high as 11·1–23·5%.[3,4] Data from population-based MRI analyses also suggest connections between normal ageing and asymptomatic stages of age-associated small-vessel diseases, such as hypertensive vasculopathy and cerebral amyloid angiopathy. Despite several comprehensive reviews of CMBs,[5–9] recent advances warrant a new assessment of emerging technical features of image acquisition, specific criteria for lesion identification, and recent data from population-based studies.

Detection of CMBs

CMBs are primarily a radiological construct (ie, small MRI signal voids), but one that is indicative of specific underlying microscopic pathological changes (ie, perivascular collections of haemosiderin deposits that are foci of past haemorrhages). Here, we review advances in MRI for the detection of CMBs, the criteria used to include or exclude MRI lesions as genuine CMBs, and what is known of the correlation between MRI and underlying histopathology. A glossary of commonly used MRI terms is provided in panel 1.

MRI parameters

The haemosiderin deposits that comprise CMBs[10] are superparamagnetic and thus have substantial internal magnetisation when in the MRI magnetic field—a property known as magnetic susceptibility. Internal magnetisation generates local inhomogeneity in the magnetic field surrounding the CMB, leading to fast decay of the local MRI signal, called the susceptibility effect. On MRI sequences that are particularly sensitive to susceptibility effects, CMBs will appear as black or hypointense lesions (ie, signal voids).

The MRI parameters with the greatest effect on detection of CMBs are pulse sequence, sequence parameters, spatial resolution, magnetic field strength, and image post-processing. The potential effect of these factors on conspicuity and detection of microbleeds is discussed below. Limited experience with various MRI parameters in population-based studies (table)[2–4,11–13] suggests that choice of methods substantially affects the reported prevalence of CMBs.

Among the available pulse sequences, T2*-weighted gradient-recalled echo (GRE) MRI without the 180° refocusing pulse characteristic of spin-echo or fast spin-echo techniques[14] is highly sensitive to the susceptibility effect. T2*-weighted GRE sequences tailored to image susceptibility effects (referred to as T2*-weighted MRI in this Review) are substantially more sensitive to CMBs than are T2-weighted spin-echo sequences.[2,15–17] Areas of low intensity on T2*-weighted MRI are larger than the actual haemosiderin deposits—the so-called blooming effect (figure 1). Because the extent of blooming varies with MRI parameters, the size of the measured signal void will depend on factors other than size of the corresponding histopathological CMB. Echo-planar GRE imaging, in which an entire image is obtained from a single radiofrequency excitation pulse, can lead to ultrafast acquisition with comparable CMB conspicuity to that of T2*-weighted MRI,[18] but possibly at the cost of increased susceptibility effects from air and bone at the skull base, poor image suppression of fatty tissue, and image distortion.[19]

The sequence parameter that most affects sensitivity to magnetic susceptibility in T2*-weighted MRI is echo time. Echo times of 25–50 ms have generally been used (table),[2,16,20] with long echo times enabling more time for dephasing, thereby enlarging the susceptibility effect.[21]

Use of long echo times, however, can compromise image quality because of decay of transverse magnetisation.[22]

Higher spatial resolution (in particular the use of thinner scanning sections) offers the possibility of minimising the partial-volume averaging that might affect detection of CMBs. Use of a three-dimensional Fourier transform technique in T2*-weighted MRI enables acquisition of thin image slices at a high signal-to-noise ratio. Recently, the use of three-dimensional T2*-weighted MRI at sub-millimetere spatial resolution (reconstructed voxel size of 0·5×0·5×0·8 mm³) detected more CMBs than did conventional two-dimensional GRE at lower resolution (figure 1).[20] In a study of imaging with different slice thicknesses from individuals with cerebral amyloid angiopathy, individual CMBs had about twice the contrast index (a measure of conspicuity) in 1·5 mm thick slices than in 5·0 mm thick slices.[23] The longer scan times associated with scanning at small voxel sizes in three-dimensional T2*-weighted MRI can be reduced to acceptable limits by use of parallel imaging.[20]

Increased magnetic field strength, to 3 Tesla (T) or higher, seems to improve CMB conspicuity.[23–26] The susceptibility effect is increased at higher magnetic field strengths, and blooming effects are therefore predicted to be greater than for lower magnetic field strengths.

Finally, the use of image post-processing techniques might further increase the contrast between brain tissue and haemosiderin deposits. T2* effects can be augmented by multiplying magnitude (indicating loss of signal) with phase (indicating haemosiderin-associated signal phase shift), a technique known as susceptibility-weighted imaging.[27] Use of susceptibility-weighted imaging of CMBs is promising,[28] giving a substantially higher contrast index for individual CMBs than does conventional T2*-weighted MRI.[23] The added value of susceptibility-weighted imaging over techniques with higher field strength and smaller voxel sizes needs to be determined.

Panel 1: Glossary of commonly used MRI terms

Dephasing is the process by which protons precess out of phase when the 90° excitation pulse is switched off. Dephasing is caused by inhomogeneities in the magnetic field that are either intrinsic (due to a single voxel containing different tissue types) or extrinsic (due to imperfections in the external magnetic field).

Echo time refers to the time in milliseconds between application of the 90° excitation pulse and the peak of the elicited echo signal.

Echo-planar imaging is a readout method in which the complete image is formed from a single radiofrequency excitation pulse. Echo-planar imaging can be used in spin-echo or fast spin-echo or in gradient-recalled echo or T2*-weighted acquisition schemes.

Fast spin-echo is a type of spin-echo technique (see below) that uses a series of rapid 180° refocusing pulses and multiple echoes (echo train) and is in standard use for T2-weighted MRI because of the shortened scan duration.

Fourier transform techniques are mathematical procedures for converting raw MRI data into image data by separating out the frequency and amplitude components of the MR signal as a function of time.

Gradient-recalled echo is an MRI pulse sequence that lacks a 180° refocusing (rephasing) pulse and is therefore more sensitive to magnetic susceptibility effects than are spin-echo or fast spin-echo techniques. Gradient-recalled echo is often used for T2*-weighted imaging.

Image post-processing refers to the application of various computerised mathematical operations to the image data to enhance particular tissue features.

Magnetic susceptibility is a tissue property of generating internal magnetisation when brought into the magnetic field of an MRI scanner.

Partial-volume averaging refers to the loss of contrast between two adjacent tissue types caused by insufficient spatial resolution. At low resolution, the two tissue types are averaged together within a single voxel rather than imaged separately.

Pulse sequences are a preselected set of parameters of MR image acquisition, including the timing, amplitude, and repetition of radiofrequency and gradient pulses.

Refocusing pulse (rephasing pulse) refers to the 180° pulses that follows the 90° excitation pulse in spin-echo or fast spin-echo sequences. The purpose of the refocusing pulse is to produce a rephasing of protons that have dephased after the 90°excitation pulse, causing them to regain coherence and produce a signal echo.

Repetition time refers to the time in milliseconds between successive radiofrequency pulse sequences applied to the same image slice. Repetition time is a major determinant of total scan time.

Signal phase shift is the loss in the phase coherence of precessing protons.

Spin-echo techniques are MRI pulse sequences in which both a 90° excitation pulse and a 180° refocusing pulse are used to generate an MR signal. The 180° refocusing pulse has the effect of decreasing magnetic susceptibility effects.

Susceptibility effect refers to the fast decay of the local MRI signal caused by the internal magnetisation of tissue that generates local inhomogeneity in the magnetic field.

Susceptibility-weighted imaging is a term applied to MRI data acquisition techniques that generate additional contrast for magnetic susceptibility by use of phase imaging combined with magnitude data in an image post-processing step.

T2*-weighted imaging refers to MRI pulse sequences that are designed to be sensitive to signal decay caused by magnetic field inhomogeneities.

Transverse magnetisation is the precession of protons in response to the 90° excitation pulse.

Voxels are units of tissue volume that correspond to the smallest three-dimensional space from which MRI data are acquired.

Lesion characteristics, mimics, and detection criteria

Although precise definitions of the MRI lesions that should be classified as CMBs have varied,[7] general agreement is that they are small areas of signal void with associated blooming, excluding larger haematomas (macrobleeds), specific secondary causes of bleeding, and non-haemorrhagic causes of signal void. This starting point leaves several unanswered questions, including how best to define the operational rules that are needed to distinguish CMBs from macrobleeds and haemorrhagic and non-haemorrhagic lesions that resemble CMBs.

Various size cut-off points have been used to classify microbleeds, with a maximum diameter of 5–10 mm and, in some studies, a minimum diameter of 2 mm.[7] However, recent insights suggest several reasons why precise size criteria should not be emphasised. First, the size of a CMB on MRI depends on imaging parameters, such as field strength and sequence. This together with the difficulty in implementing identical pulse sequences on different MRI systems substantially complicates comparison of CMB size across studies. Second, microbleeds and macrobleeds might have a naturally bimodal size distribution that does not strongly depend on the precise cut-off point chosen. A recent analysis of lesion volumes of 163 haemorrhages seen on routine clinical (1·5 T, 5 mm slice thickness) T2*-weighted MRI among 46 individuals presenting with probable cerebral amyloid angiopathy did not find a single continuum of haemorrhage sizes; instead, a distinctly bimodal distribution with separate widely spaced peaks for microbleeds and macrobleeds was seen.[29] The cut-off point that best divided the microbleed and macrobleed peaks was a diameter of 5·7 mm,[29] which falls within the maximum size of 5–10 mm conventionally used.[5–7]

The sensitivity of T2*-weighted MRI to paramagnetic substances other than haemosiderin, including calcifications, iron deposits, or deoxyhaemoglobin, gives rise to findings that resemble CMBs (CMB mimics). Such artifacts are likely to be more of a problem when using methods with high sensitivity to magnetic susceptibility such as susceptibility-weighted MRI or high-field strength MRI.

Both calcium and iron deposits can appear as small foci of low signal intensity on T2*-weighted MRI (figure 2). These abnormalities are usually found bilaterally in the basal ganglia, although calcification can also occur in the choroid plexus, the pineal gland, and lobar locations. CT can facilitate identification of suspected calcification, although its routine use is rare (used in six of 53 reviewed studies).[7]

Flow voids in pial blood vessels seen in cross-section in cortical sulci can be distinguished from CMBs by their location, their equal visibility on T2-weighted spin-echo and GRE sequences (as arterial flow voids do not generate a blooming effect), and their linear structure when examined over contiguous slices, which is particularly evident in thin slices. Paramagnetic deoxyhaemoglobin in cerebral venules produces its own blooming effect; however, the tubular structure of these venules distinguishes them from CMBs (figure 2). The distinction from flow voids can also be difficult if a CMB is adjacent to a small vessel; in this case, the lesion's termination as a blind end rather than its linear continuation as a vessel branch should be indicative of a CMB.

Partial volume artifact from bone (with associated susceptibility artifact from air in the sinuses) might obscure CMBs or confuse their interpretation, particularly in the temporal and frontal lobes because of the orbit and mastoid bones (figure 2).

Cavernous malformations can be thought of as secondary causes of CMBs (particularly the small type IV cavernous malformations[30]). These malformations are distinguishable from typical primary CMBs by T1-weighted and T2-weighted sequences showing stagnant blood in the sinusoidal lumen, extravasated

	Participants		MRI parameters					Microbleeds	
	n	Mean age in years (standard deviation)	Sequence	Field strength (Tesla)	Echo time (ms)	Section thickness (mm)	In-plane resolution (mm)	Prevalence (%)	Associated factors
Austrian Stroke Prevention Study[2]	280	60 (6)	2D T2* GRE	1·5	16–20	5 (10% gap)	Not available	6·4	Age, hypertension, systolic and diastolic blood pressure, lacunar infarcts, white matter lesions
Japanese study[11]	450	53 (8)	2D T2* GRE	1·0	30	5 (2·5 mm gap)	0·9×1·1	3·1	Hypertension, heavy smoking
Japanese brain docking study[12]	209	56 (8)	2D T2* GRE	1·5	26	8 (no gap)	0·9×1·2	7·7	Age, hypertension, headache
Framingham Study[13]	472	64 (12)	2D T2* GRE	1·0	26	5 (10% gap)	Not available	4·7	Age, male sex
AGES Reykjavik Study[3]	1962	76 (6)	2D T2* GRE-EPI	1·5	50	3 (no gap)	0·9×0·9	11·1	Age, male sex, *APOE* ε4/ε4, retinal lesions, diabetes
Rotterdam Scan Study[4]	1062	70 (7)	3D T2* GRE	1·5	31	1·6 (zero-padded to 0·8 mm; no gap)	0·8×0·8	23·5	Age, systolic blood pressure, pulse pressure, smoking, low cholesterol, *APOE* ε4/–, lacunar infarcts, white matter lesions

2D=2-dimensional. 3D=3-dimensional. AGES Reykjavik Study=Age, Gene/Environment Susceptibility. APOE=apolipoprotein E genotype. EPI=echo-planar imaging. GRE=gradient-recalled echo.

Table: **Population-based studies of cerebral microbleeds**

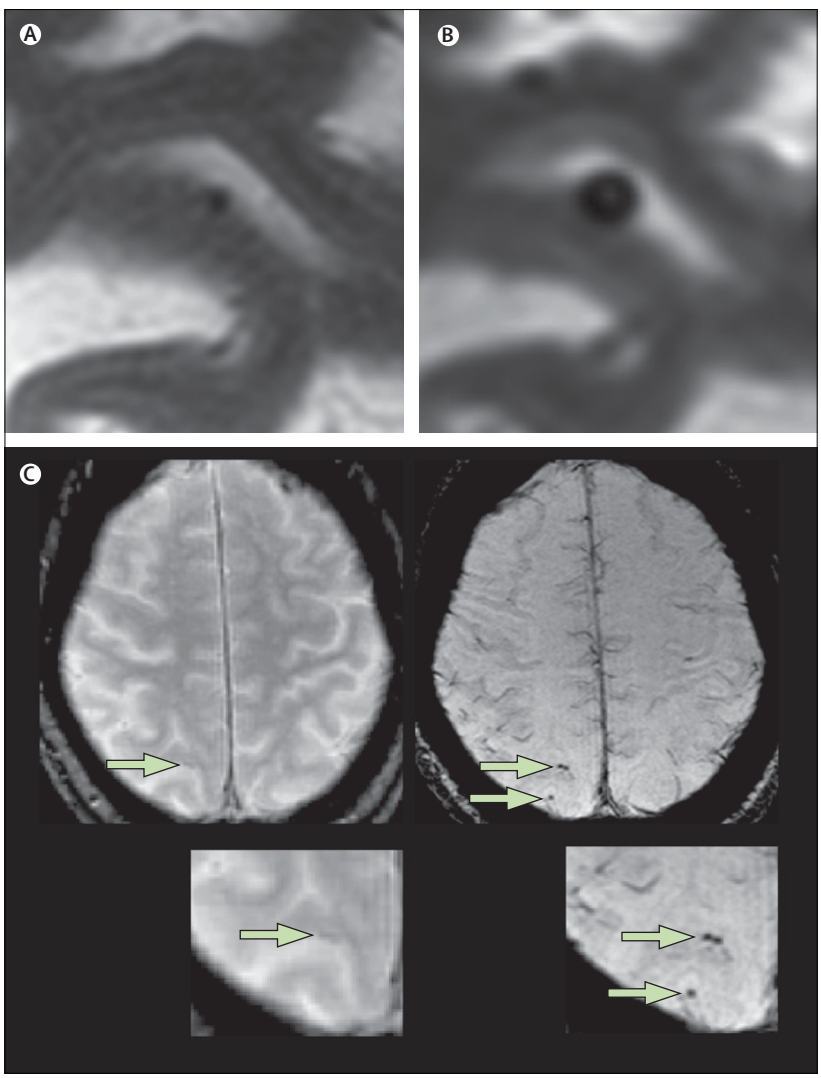

Figure 1: **Increased conspicuity of CMBs with T2*-weighted MRI techniques**
T2 fast SE (A) and T2*-weighted GRE MRI (B) of the same CMBs, shown at high magnification, are compared. The blooming effect is shown by the larger area of signal void on the T2*-weighted MRI compared with the fast SE image. The GRE image also shows the ringing artifact as an area of high signal within the signal void. (C) Images obtained at corresponding axial levels by use of a conventional 2D T2*-weighted MRI sequence (left panel; TR/TE 775/20, flip angle 25°, voxel size 0·5×0·5×5 mm³) are compared with an accelerated 3D T2*-weighted MRI sequence (right panel; TR/TE 45/31, flip angle 13°, voxel size 0·5×0·5×0·8 mm³). Magnifications of matching brain regions are shown at the bottom. The 3D T2*-weighted MRI scan shows three CMBs in lobar locations (white arrows) that are not, or are barely, discernible on the 2D T2*-weighted MRI scan. 2D=two-dimensional. 3D=three-dimensional. CMB=cerebral microbleed. GRE=gradient-recalled echo. SE=spin-echo. TE=echo time. TR=repetition time.

blood at varying stages of degradation, and a characteristic haemosiderin rim[31] (figure 2). This CMB mimic can itself look like the ringing artifact seen on T2*-weighted MRI (figure 1A), indicating increased signal within a flow void. Ringing artifact is typically absent on T2-weighted spin-echo MRI, which emphasises the importance of combining spin-echo with T2*-weighted MRI.

Metastatic melanoma in the brain can appear as a hypointense area on T2*-weighted MRI,[32] a result of both the presence of melanin and the tendency of these tumours to bleed. In many cases, these lesions can be distinguished from primary CMBs by the concomitant presence of T1 hyperintensity (caused by the melanin) or of surrounding oedema (particularly after recent intratumour haemorrhage); however, small non-oedematous lesions might resemble primary CMBs.

Diffuse axonal injury after head trauma is another potential secondary cause of CMBs, distinguishable from primary CMBs by the clinical history and concomitant imaging abnormalities.[33]

On the basis of the above considerations, we suggest criteria for CMB detection (panel 2). For designation as a CMB, a signal should be black or substantially hypointense on T2*-weighted MRI, round or ovoid (excluding tubular or linear structures such as those indicating vessels or a resorbed macrobleed), blooming (larger or more conspicuous on GRE than on spin-echo MRI), devoid of T1-weighted or T2-weighted hyperintensity (such as cavernous malformation, haemorrhagic infarct, or melanotic melanoma), and at least half surrounded by brain parenchyma (to include superficial CMBs as seen in individuals with cerebral amyloid angiopathy). Other mimics of CMBs, such as mineralisation of the basal ganglia or diffuse axonal injury, are excluded on the basis of appearance or clinical history. Size should be used conservatively, if at all, in the identification of CMBs.

A consequence of the differential diagnosis of CMBs is disagreement among raters about their presence and numbers. Inter-rater correlation coefficients for the numbers of CMBs are more than 0·8, but inter-rater agreement on the presence of one or more CMBs in studies with conventional T2*-weighted MRI vary (κ 0·33–0·88),[34] probably because of difficulties in detection and certainty about one or a few lesions. Early investigations suggest that standardised rating instruments might improve inter-rater reliability.[34]

Radiological-pathological correlation

In addition to the imaging artifacts described above, MRI has limitations compared with histopathological examination for investigating CMBs, including an inability to provide microscopic evidence for specific tissue or small-vessel pathological changes. However, histopathology has its own limitations, particularly the fact that examination of the entire brain in microscopic section is not practically possible. This limitation is particularly relevant to identification of CMB lesions that are near the lower limits of gross visual detection and small enough to be fully contained within even a thin (eg, 5 mm) brain slice, which prevents them from being visible to the examining pathologist. Conversely, the ability of modern MRI techniques to sample the whole brain at spatial resolutions of 1 mm or less raises the possibility that MRI might ultimately prove substantially more sensitive than histopathology for CMB detection.

Studies of the radiological-pathological correlation of CMBs[10,35,36] have shown a link between most signal voids seen on T2*-weighted MRI and microscopic haemorrhagic foci. Fazekas and co-workers[10] have reported that 21 hypointense lesions seen on T2*-weighted MRI of 11 autopsied brains corresponded pathologically to clusters of haemosiderin-laden macrophages. Tatsumi and co-workers[36] reported similar pathological findings in eight of nine T2*-weighted MRI hypointense lesions identified in post-mortem brain slices of a single brain.

In these studies of conventional T2*-weighted MRI methods, sensitivities of MRI and histopathological examination for CMB detection seemed similar. In the study by Fazekas and co-workers,[10] T2*-weighted MRI (with 5 mm slices and a 0·5 mm inter-slice gap) showed 13 lesions not seen on histopathological examination, whereas 20 further CMBs that were not detected by T2*-weighted MRI were identified on histopathological examination. These MRI-negative lesions tended to be smaller than the MRI-positive lesions (described as "only a few perivascular haemosiderin-laden macrophages") and, in retrospect, might be the CMBs now seen with more sensitive T2*-weighted methods. Further radiological-pathological correlation studies with these more sensitive imaging methods will be needed to determine whether these techniques indeed show a higher proportion of histopathological microbleeds than seen with conventional T2*-weighted MRI.

The specificity of T2*-weighted MRI for CMBs seems to be high. Among the 14 MRI lesions that were not identified as histopathological microbleeds in the studies by Fazekas and colleagues and Tatsumi and colleagues,[10,36] only one was a potential radiographic mimic of CMB, described as a vascular pseudocalcification.[36] Use of newer T2*-weighted MRI methods to repeat these correlation analyses will be important to confirm that the sensitive imaging techniques maintain a high specificity for CMBs.

Interpretation of CMBs

Markers of disease

Vascular pathological changes

One approach to the interpretation of CMBs is to regard them as a marker of accompanying vascular pathological change. Histopathological analyses of the vessels associated with CMBs, done primarily in brains with haemorrhagic stroke, have generally identified two types of vascular pathological changes: hypertensive vasculopathy and cerebral amyloid angiopathy.[10,35,37] For example, among the 11 brains examined by Fazekas and co-workers,[10] advanced hypertensive lipohyalinotic changes were seen in nine and cerebral amyloid angiopathy in two brains. These two disorders are characterised by different patterns of microbleed distribution: hypertensive vasculopathy is typically associated with CMBs in the basal ganglia, thalamus, brainstem, and cerebellum,[10] whereas advanced cerebral amyloid angiopathy is associated with a lobar (or, less commonly, cerebellar) distribution (figure 3).[37] The lobar distribution in cerebral amyloid angiopathy is consistent with the distribution of vascular pathological changes[38]

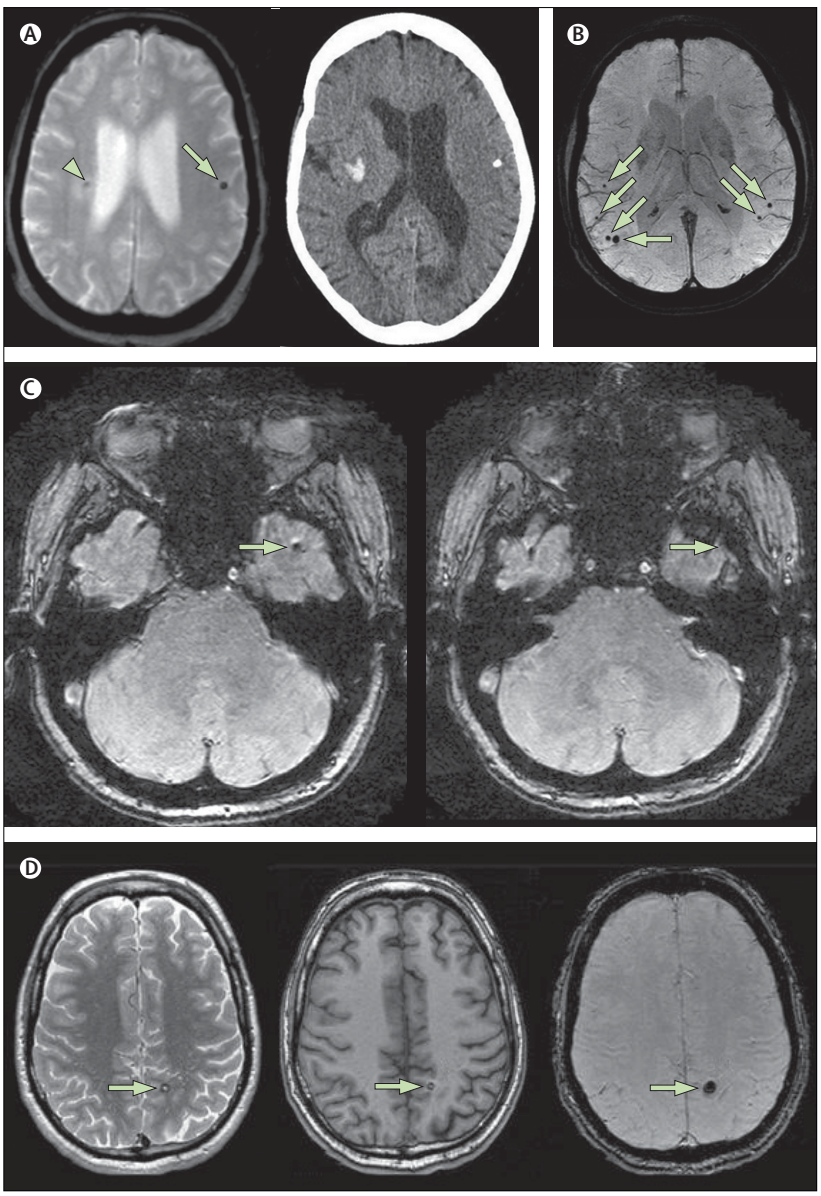

Figure 2: **CMB confounds and mimics**
(A) An axial T2*-weighted MRI scan shows a calcification in the left hemisphere (left panel; arrow) resembling a CMB. The CT scan shows this lesion as an area of high density (right panel). Note that the MRI scan also shows a right hemispheric hypointense lesion (arrowhead) surrounded by hyperintense signal, corresponding to the tip of a spontaneous intracerebral haemorrhage shown on the CT image. (B) A minimum intensity projection of an axial T2*-weighted MRI scan (4 mm slice) shows CMBs (arrows) in proximity to vessel flow voids on the brain surface. The vessels can be distinguished from CMBs by their linear shape, whereas the CMBs appear as blind-ended round or ovoid structures. (C) An axial T2*-weighted MRI scan shows partial volume artifact as a potential CMB mimic. The axial T2*-weighted MRI scan (left panel) shows a round focus of signal loss (arrow) that could be interpreted as a left temporal CMB. The image just caudal to this (right panel) indicates that this hypointensity is due to partial volume artifact from the adjacent left sphenoid bone (arrow). (D) Axial proton density-weighted (left panel), T1-weighted (middle panel), and T2*-weighted (right panel) MRI scans depict a cavernous malformation (arrows) resembling a CMB. The hyperintense signal within the hypointense rim on proton density or T2-weighted sequences helps distinguish these lesions from CMBs. CMB=cerebral microbleed.

***Panel 2:* Recommended criteria for identification of cerebral microbleeds**

- Black lesions on T2*-weighted MRI
- Round or ovoid lesions (rather than linear)
- Blooming effect on T2*-weighted MRI
- Devoid of signal hyperintensity on T1-weighted or T2-weighted sequences
- At least half of lesion surrounded by brain parenchyma
- Distinct from other potential mimics such as iron or calcium deposits, bone, or vessel flow voids
- Clinical history excluding traumatic diffuse axonal injury

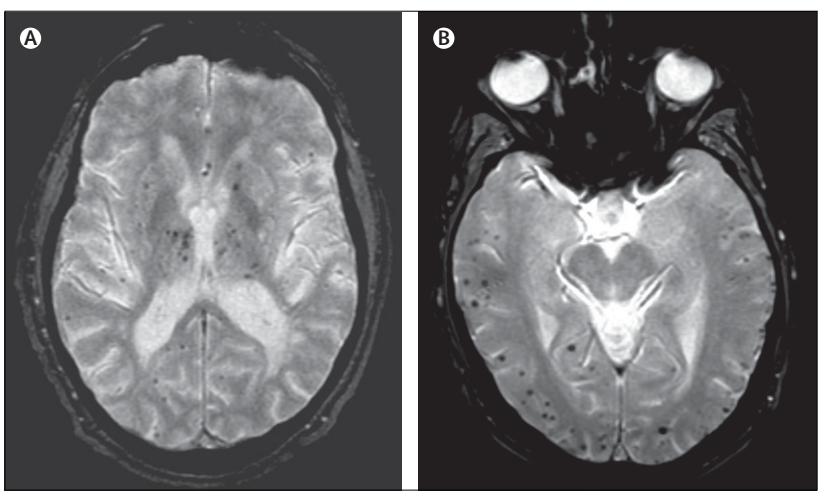

Figure 3: **Deep hemispheric and isolated lobar patterns of CMB distribution**
(A) A T2*-weighted MRI scan from an 84-year-old woman with long-standing hypertension. CMBs are present predominantly in the bilateral thalamus, putamen, caudate, and cerebellum, with only a small number in lobar brain regions (not shown in this image). (B) A T2*-weighted MRI scan from a 77-year-old woman without hypertension. CMBs are present only in lobar brain regions, meeting criteria for probable cerebral amyloid angiopathy.[37] CMB=cerebral microbleed.

and has served as the basis for the radiological diagnosis of probable cerebral amyloid angiopathy by use of the Boston criteria in patients with haemorrhagic stroke.[37] These pathologically validated Boston criteria specify that the diagnosis of probable cerebral amyloid angiopathy cannot be made if any CMBs are located in the basal ganglia, thalamus, or brainstem—regions that are atypical for pathological changes in this disorder. Within the lobar brain compartment, cerebral amyloid angiopathy-associated CMBs[39] and the underlying cerebral amyloid angiopathy pathological changes[38,40] seem to favour posterior cortical regions, particularly the occipital lobe.

The pathological factors that determine whether a particular bleeding event will result in a microbleed versus a macrobleed is another focus of continuing investigation. The observed bimodal distribution of haemorrhagic volumes[29] raises the possibility of a threshold mechanism, whereby a bleed can either remain small or reach a crucial size that causes it to continue to enlarge fully into the macrobleed range. This possibility echoes Fisher's suggestion in 1971 that macrobleeds occur in avalanche or domino style[41]—when bleeding from one ruptured vessel causes secondary rupture of surrounding arteries. Fisher based this idea on the observation that a serially sectioned acute hypertensive pontine haemorrhage was surrounded by 24 or more sites of recent arterial rupture in vessels without advanced lipohyalinotic changes, which seemed to be sites of mechanical rupture secondary to the primary bleed. This classic study offers a framework for future investigations of how CMBs might be associated with their larger symptomatic counterparts.

Association with disease-associated risk factors

A second approach to CMB interpretation is analysis of their associations with particular risk factors and disease states. Studies of factors associated with CMBs in patients with haemorrhagic stroke or ischaemic stroke and in community-dwelling elderly individuals (table) have been extensively reviewed.[5–7] Hypertension is the most consistent predictor of CMBs, with odds ratios averaged across studies in patients with stroke and healthy adults of 2·3 and 3·9, respectively.[7] An association between CMBs and hypertension is further supported by studies of their relation to recorded blood pressures,[2,4] lacunar infarcts or white matter lesions,[2,4,13,42–48] retinal microvascular lesions,[49] and left-ventricular hypertrophy.[50] These observations suggest that the blood pressure-associated vascular pathological changes that can cause larger, symptomatic intracerebral haemorrhage can also give rise to CMBs. Other risk factors for intracerebral haemorrhage such as age[2–4,12,13] and low serum cholesterol concentrations[4,51] also seem to be associated with a high prevalence or number of CMBs. The association between low cholesterol concentrations and CMBs is particularly interesting in light of recent data showing increased risk of symptomatic intracerebral haemorrhage in patients with stroke randomly assigned to high-dose atorvastatin.[52] However, this increased risk was independent of low-density lipoprotein cholesterol concentration,[53] suggesting causes other than lipid lowering.

Recent population-based data support the possibility that CMB location (deep hemispheric or infratentorial versus strictly lobar) might relate to specific underlying vascular pathological changes. Analysis of the *APOE* genotype in individuals from the Rotterdam Scan Study grouped by CMB distribution showed an association of the *APOE* ε4 allelle with isolated lobar CMBs (odds ratio for *APOE* ε4 carriers of 1·87; 95% CI 1·25–2·81) but not with deep hemispheric or infratentorial CMBs (1·17; 0·70–1·93).[4] Given the relation between *APOE* ε4 and cerebral amyloid angiopathy,[54,55] these results raise the possibility that individuals with isolated lobar CMBs (58% of CMB-positive people in the Rotterdam study[4]) might have advanced cerebral amyloid angiopathy. In the same study, systolic blood pressure, severe hypertension, and lacunar infarcts were more closely linked to deep or infratentorial CMBs,[4] suggesting hypertensive vasculopathy as the predominant

underlying disease in this subgroup. These findings still await confirmation from other population-based studies of elderly people. The Framingham Study of younger participants (mean age 64 years) scanned at a lower magnetic field strength (table) found no association with *APOE* genotype among all CMBs or in participants with lobar-only CMBs,[13] whereas the Age, Gene/Environment Susceptibility (AGES) Reykjavik Study of older people (mean age 76 years) reported a significant over-representation of *APOE* ε4 homozygotes among all people with CMBs (4·2% *vs* 1·8%; p=0·01).[3]

Determining whether a lobar distribution of CMBs can be used to diagnose cerebral amyloid angiopathy in the general population might ultimately require population-based MRI–autopsy correlation studies. Previously reported population-based, clinical autopsy series have shown cerebral amyloid angiopathy to be a common neuropathological finding,[40,56,57] but have not yet been used to examine the relation between cerebral amyloid angiopathy and CMBs detected on pre-mortem MRI.

Risk for haemorrhagic stroke

As markers of underlying haemorrhage-prone vascular pathological changes, CMBs might predict future risk of symptomatic intracerebral haemorrhage. Studies of patients who had had lobar intracerebral haemorrhage[58] or ischaemic stroke[59] and who were prospectively followed up suggest that this is the case, at least after stroke. Among 94 patients who had had primary lobar haemorrhage, high total numbers of haemorrhages (the presenting intracerebral haemorrhage plus other microbleeds and macrobleeds detected by T2*-weighted MRI at baseline) predicted increased risk of future symptomatic haemorrhage: the 3-year cumulative risk was 14% for patients who had only one haemorrhage, 17% for two, 38% for three to five, and 51% for six or more haemorrhages.[58] Similarly, among 908 people who had had ischaemic stroke, the risk of subsequent haemorrhagic stroke over 26 months of follow-up increased from 0·6% for those with no accompanying CMB to 1·9% with one, 4·6% with two to four, and 7·6% for five or more CMBs.[59] Studies of patients who have had ischaemic stroke have also indicated possible links between CMBs and spontaneous or thrombolysis-associated bleeding after stroke (primarily into the infarcted territory),[60,61] although these findings have been called into question by recent analyses.[62,63] The predictive value of CMBs in people without previous stroke is unknown and is a key concern for longitudinal population studies in progress.

The association between CMBs and future symptomatic intracerebral haemorrhage raises the question of whether the increased risk might be enough to move the risk–benefit calculation away from anticoagulation in situations in which it would otherwise be beneficial, such as for the prevention of thromboembolism in individuals with atrial fibrillation. A recent decision analysis with current risk estimates suggested that anticoagulation would still be beneficial in people with asymptomatic CMBs,[64] which contrasts with the suggestion that anticoagulation should be avoided after symptomatic intracerebral haemorrhage associated with cerebral amyloid angiopathy.[65] With regard to antiplatelet therapy, longitudinal data from 127 patients with symptomatic lobar intracerebral haemorrhage (27 on antiplatelet drugs) and 80 patients with symptomatic deep hemispheric intracerebral haemorrhage (19 on antiplatelet drugs) did not show an increase in recurrent intracerebral haemorrhage associated with antiplatelet therapy, although a slightly higher risk relative to untreated patients could not be excluded.[66] The question of how CMBs should affect antithrombotic use is an active area of investigation, particularly in light of broadening indications for these compounds.

Contributors to neurological dysfunction

In addition to the use of CMBs as markers of underlying disease, they could also have direct effects on neurological function, cognition, and disability. Neuropathological analyses of CMBs generally indicate that these lesions are associated with surrounding tissue damage,[10,35,36] suggesting a potential mechanism for brain dysfunction.

The possibility that CMBs contribute to clinical deficits is supported by findings from a prospective study of 94 patients who had had primary lobar intracerebral haemorrhages.[58] A high number of haemorrhages at baseline was associated with a high risk of cognitive impairment, functional dependence, or death: the 3-year cumulative risk was 16% for patients with one haemorrhage, 20% for two, 51% for three to five, and 52% for six or more haemorrhages. CMBs have also been associated with clinical disability in the hereditary small-vessel disease CADASIL (cerebral autosomal dominant arteriopathy with subcortical infarcts and leucoencephalopathy).[67,68] In a two-centre cohort study of 147 patients with CADASIL, the number of CMBs was independently associated with functional dependence (defined as a modified Rankin score of ≥3) with an odds ratio per further microbleed of 1·16 (95% CI 1·01–1·34; p=0·034) after adjustment for confounding variables.[68] Multivariable analysis to define correlates of cognition did not, however, show a similar independent association with CMBs. Finally, a small case–control study of patients with ischaemic stroke or transient ischaemic attack showed that individuals with CMBs did worse on standard tests of executive function than did those without microbleeds.[69] Although each of these studies attempted to control for potential confounders, the association of CMBs with other markers of small-vessel injury, such as lacunar infarcts and white matter damage, indicates the need for confirmation in larger studies with greater statistical power and studies of individuals without stroke.

If CMBs do have direct effects on brain function (rather than simply marking the presence of other cerebrovascular pathological changes), one would expect the location of CMBs to play a part. In analyses of the two-centre CADASIL cohort, CMBs in the caudate nucleus were independently associated with low global cognitive scores (on the basis of the Mattis dementia rating scale; p=0·027) and CMBs in the frontal lobes showed a trend towards lower global cognitive scores (p=0·056) compared with all other patients with CADASIL (with or without CMBs).[70] Similarly, a small study of 55 patients with stroke or transient ischaemic attack suggested that there were more microbleeds in the frontal lobes and basal ganglia of those with executive dysfunction than in those without.[69] Detailed anatomical mapping of CMBs, as has been done with other MRI lesions,[71] is a promising approach for future correlation studies relating clinical and MRI findings. However, given the widespread distribution of CMBs and their frequent association with other small vessel-associated pathological changes, such studies will need to be both large and carefully controlled.

Recommendations and future directions

CMBs are a well defined pathological lesion that can be detected by use of T2*-weighted MRI techniques with high sensitivity (particularly by use of new methods), high reliability (with careful image interpretation and consideration of CMB mimics), and high specificity (proven for conventional T2*-weighted MRI, still to be established for the newer methods). The full brain coverage by MRI probably renders neuroimaging a more sensitive method for CMB detection than are histopathological techniques.

The choice of T2*-weighted MRI method (including sequence parameters, spatial resolution, field strength, and image post-processing) affects the number of CMBs detected and, thus, overall study sensitivity. Although specification of a standard sequence for all future studies is premature, such a standard will be developed over the coming years and will probably include imaging of thin slices. Reaching a common standard will be facilitated by further side-by-side comparisons of individuals with CMBs imaged by use of different MRI methods.[20,23]

All studies of CMBs should specify the above imaging parameters and should follow systematic rules or standardised rating instruments for excluding CMB mimics. These factors should presumably be held constant in longitudinal studies with repeated measurements. The choice of precise size parameters for CMBs does not seem to have a major effect on the detection of microbleeds.

By use of advanced T2*-weighted MRI methods, population-based studies have shown CMBs to be common in community-dwelling elderly people, with prevalences between 10% and 25%. Accumulating evidence suggests that CMBs might indicate specific underlying vascular pathological states, in particular hypertensive vasculopathy (for CMBs in deep hemispheric or infratentorial locations) or cerebral amyloid angiopathy (for CMBs restricted to lobar locations). The presence and number of CMBs might also indicate the severity of these haemorrhage-prone pathological states and predict the risk of future symptomatic intracerebral haemorrhage. Future studies of people with CMBs should include analyses of subgroups divided according to CMB location (deep hemispheric or infratentorial *vs* lobar only; figure 3).

Whether CMBs directly disrupt brain functioning is unclear and carefully controlled studies are needed to disentangle their contribution from that of other small-vessel brain lesions, such as lacunar infarcts and white matter hyperintensities, that accompany CMBs in many people.

The immediate future of CMB research will probably see development of a shared set of standards for the detection of microbleeds that will enable informative cross-study comparisons and robust longitudinal data collection. Determining whether CMBs should affect clinical decision making, identifying their inter-relation with other signs of small-vessel disease, and describing their independent contribution to vascular cognitive and neurological dysfunction are key long-term goals.

Search strategy and selection criteria

The content of this Review is based on the group consensus from a conference entitled "Cerebral Microbleeds: Detection and Definition". Additional references for this Review were identified through searches of PubMed with the search terms "microbleed(s)", "microh(a)emorrhage(s)", or "petechial h(a)emorrhage(s)"; or "gradient-echo", "T2*", or "susceptibility" in conjunction with "h(a)emorrhage(s)", from January, 1966 to October, 2008. References were also identified from the bibliography of identified articles and the authors' files. Only papers published in English or with available English translations of relevant data were reviewed. The final reference list was generated on the basis of relevance to the topics covered in this Review.

Contributors

SMG organised the conference that formed the basis of the content of this Review, drafted the text, and prepared the figures. MWV, CC, and MAVB drafted the text and prepared the figures. AV drafted the text. MMBB co-organised the consensus conference. All authors made crucial revisions to the paper.

Conflicts of interest

We have no conflicts of interest.

Acknowledgments

Other members of the Microbleed Study Group who participated in the Cerebral Microbleeds: Detection and Definition conference and contributed valuable discussions and criticisms for this paper were M A Ikram, M J Bos, M M F Poels (Rotterdam, Netherlands), J van der Grond (Leiden, Netherlands), M E Gurol, and R N K Nandigam (Boston, USA). The conference was held by the Microbleed Study Group on April 12, 2008 in Chicago, USA and was supported by sundry research funds provided by individual donors to the Massachusetts General Hospital Hemorrhagic Stroke Research Program without commercial interests or contributions from industry.

References

1 Offenbacher H, Fazekas F, Schmidt R, Koch M, Fazekas G, Kapeller P. MR of cerebral abnormalities concomitant with primary intracerebral hematomas. *AJNR Am J Neuroradiol* 1996; **17:** 573–78.

2 Roob G, Schmidt R, Kapeller P, Lechner A, Hartung HP, Fazekas F. MRI evidence of past cerebral microbleeds in a healthy elderly population. *Neurology* 1999; **52:** 991–94.

3 Sveinbjornsdottir S, Sigurdsson S, Aspelund T, et al. Cerebral microbleeds in the population based AGES Reykjavik study: prevalence and location. *J Neurol Neurosurg Psychiatry* 2008; **79:** 1002–06.

4 Vernooij MW, van der Lugt A, Ikram MA, et al. Prevalence and risk factors of cerebral microbleeds: the Rotterdam Scan Study. *Neurology* 2008; **70:** 1208–14.

5 Koennecke HC. Cerebral microbleeds on MRI: prevalence, associations, and potential clinical implications. *Neurology* 2006; **66:** 165–71.

6 Viswanathan A, Chabriat H. Cerebral microhemorrhage. *Stroke* 2006; **37:** 550–55.

7 Cordonnier C, Al-Shahi Salman R, Wardlaw J. Spontaneous brain microbleeds: systematic review, subgroup analyses and standards for study design and reporting. *Brain* 2007; **130:** 1988–2003.

8 Fiehler J. Cerebral microbleeds: old leaks and new haemorrhages. *Int J Stroke* 2006; **1:** 122–30.

9 Werring DJ. Cerebral microbleeds: clinical and pathophysiological significance. *J Neuroimaging* 2007; **17:** 193–203.

10 Fazekas F, Kleinert R, Roob G, et al. Histopathologic analysis of foci of signal loss on gradient-echo T2*-weighted MR images in patients with spontaneous intracerebral hemorrhage: evidence of microangiopathy-related microbleeds. *AJNR Am J Neuroradiol* 1999; **20:** 637–42.

11 Tsushima Y, Tanizaki Y, Aoki J, Endo K. MR detection of microhemorrhages in neurologically healthy adults. *Neuroradiology* 2002; **44:** 31–36.

12 Horita Y, Imaizumi T, Niwa J, et al. Analysis of dot-like hemosiderin spots using brain dock system. *No Shinkei Geka* 2003; **31:** 263–67 [in Japanese].

13 Jeerakathil T, Wolf PA, Beiser A, et al. Cerebral microbleeds: prevalence and associations with cardiovascular risk factors in the Framingham Study. *Stroke* 2004; **35:** 1831–35.

14 Jones KM, Mulkern RV, Schwartz RB, Oshio K, Barnes PD, Jolesz FA. Fast spin-echo MR imaging of the brain and spine: current concepts. *AJR Am J Roentgenol* 1992; **158:** 1313–20.

15 Atlas SW, Mark AS, Grossman RI, Gomori JM. Intracranial hemorrhage: gradient-echo MR imaging at 1.5 T. Comparison with spin-echo imaging and clinical applications. *Radiology* 1988; **168:** 803–07.

16 Greenberg SM, Finklestein SP, Schaefer PW. Petechial hemorrhages accompanying lobar hemorrhage: detection by gradient-echo MRI. *Neurology* 1996; **46:** 1751–54.

17 Hermier M, Nighoghossian N, Derex L, et al. MRI of acute post-ischemic cerebral hemorrhage in stroke patients: diagnosis with T2*-weighted gradient-echo sequences. *Neuroradiology* 2001; **43:** 809–15.

18 Kinoshita T, Okudera T, Tamura H, Ogawa T, Hatazawa J. Assessment of lacunar hemorrhage associated with hypertensive stroke by echo-planar gradient-echo T2*-weighted MRI. *Stroke* 2000; **31:** 1646–50.

19 Liang L, Korogi Y, Sugahara T, et al. Detection of intracranial hemorrhage with susceptibility-weighted MR sequences. *AJNR Am J Neuroradiol* 1999; **20:** 1527–34.

20 Vernooij MW, Ikram MA, Wielopolski PA, Krestin GP, Breteler MM, van der Lugt A. Cerebral microbleeds: accelerated 3D T2*-weighted GRE MR imaging versus conventional 2D T2*-weighted GRE MR imaging for detection. *Radiology* 2008; **248:** 272–77.

21 Tatsumi S, Ayaki T, Shinohara M, Yamamoto T. Type of gradient recalled-echo sequence results in size and number change of cerebral microbleeds. *AJNR Am J Neuroradiol* 2008; **29:** e13.

22 Henkelman M, Kucharczyk W. Optimization of gradient-echo MR for calcium detection. *AJNR Am J Neuroradiol* 1994; **15:** 465–72.

23 Nandigam RNK, Viswanathan A, Delgado P, et al. MR imaging detection of cerebral microbleeds: effect of susceptibility-weighted imaging, section thickness, and field strength. *AJNR Am J Neuroradiol* 2008; published online November 11. DOI:10.3174/ajnr.A1355.

24 Kikuta K, Takagi Y, Nozaki K, et al. Asymptomatic microbleeds in moyamoya disease: T2*-weighted gradient-echo magnetic resonance imaging study. *J Neurosurg* 2005; **102:** 470–75.

25 Scheid R, Ott DV, Roth H, Schroeter ML, von Cramon DY. Comparative magnetic resonance imaging at 1.5 and 3 Tesla for the evaluation of traumatic microbleeds. *J Neurotrauma* 2007; **24:** 1811–16.

26 Stehling C, Wersching H, Kloska SP, et al. Detection of asymptomatic cerebral microbleeds a comparative study at 1.5 and 3.0 T. *Acad Radiol* 2008; **15:** 895–900.

27 Haacke EM, Xu Y, Cheng YC, Reichenbach JR. Susceptibility weighted imaging (SWI). *Magn Reson Med* 2004; **52:** 612–18.

28 Akter M, Hirai T, Hiai Y, et al. Detection of hemorrhagic hypointense foci in the brain on susceptibility-weighted imaging clinical and phantom studies. *Acad Radiol* 2007; **14:** 1011–19.

29 Greenberg SM, Nandigam RNK, Delgado P, et al. Microbleeds versus macrobleeds: evidence for distinct processes. *Stroke* 2008; **39:** 528.

30 Zabramski JM, Wascher TM, Spetzler RF, et al. The natural history of familial cavernous malformations: results of an ongoing study. *J Neurosurg* 1994; **80:** 422–32.

31 Al-Shahi Salman R, Berg MLM, Awad IA; on behalf of the Angioma Alliance Scientific Advisory Board. Hemorrhage from cavernous malformations of the brain: definition and reporting standards. *Stroke* 2008; **39:** 3222–30.

32 Gaviani P, Mullins ME, Braga TA, et al. Improved detection of metastatic melanoma by T2*-weighted imaging. *AJNR Am J Neuroradiol* 2006; **27:** 605–08.

33 Mittl RL, Grossman RI, Hiehle JF, et al. Prevalence of MR evidence of diffuse axonal injury in patients with mild head injury and normal head CT findings. *AJNR Am J Neuroradiol* 1994; **15:** 1583–89.

34 Cordonnier C, Potter GM, Jackson CA, et al. Improving inter-rater agreement about brain microbleeds: development of the Brain Observer MicroBleed Scale (BOMBS). *Stroke* 2009; **40:** 94–99.

35 Tanaka A, Ueno Y, Nakayama Y, Takano K, Takebayashi S. Small chronic hemorrhages and ischemic lesions in association with spontaneous intracerebral hematomas. *Stroke* 1999; **30:** 1637–42.

36 Tatsumi S, Shinohara M, Yamamoto T. Direct comparison of histology of microbleeds with postmortem MR images: a case report. *Cerebrovasc Dis* 2008; **26:** 142–46.

37 Knudsen KA, Rosand J, Karluk D, Greenberg SM. Clinical diagnosis of cerebral amyloid angiopathy: validation of the Boston criteria. *Neurology* 2001; **56:** 537–39.

38 Vinters HV, Gilbert JJ. Cerebral amyloid angiopathy: incidence and complications in the aging brain. II. The distribution of amyloid vascular changes. *Stroke* 1983; **14:** 924–28.

39 Rosand J, Muzikansky A, Kumar A, et al. Spatial clustering of hemorrhages in probable cerebral amyloid angiopathy. *Ann Neurol* 2005; **58:** 459–62.

40 Pfeifer LA, White LR, Ross GW, Petrovitch H, Launer LJ. Cerebral amyloid angiopathy and cognitive function: the HAAS autopsy study. *Neurology* 2002; **58:** 1629–34.

41 Fisher CM. Pathological observations in hypertensive cerebral hemorrhage. *J Neuropathol Exp Neurol* 1971; **30:** 536–50.

42 Kato H, Izumiyama M, Izumiyama K, Takahashi A, Itoyama Y. Silent cerebral microbleeds on T2*-weighted MRI: correlation with stroke subtype, stroke recurrence, and leukoaraiosis. *Stroke* 2002; **33:** 1536–40.

43 Naka H, Nomura E, Wakabayashi S, et al. Frequency of asymptomatic microbleeds on T2*-weighted MR images of patients with recurrent stroke: association with combination of stroke subtypes and leukoaraiosis. *AJNR Am J Neuroradiol* 2004; **25:** 714–19.

44 Imaizumi T, Horita Y, Chiba M, Hashimoto Y, Honma T, Niwa J. Dot-like hemosiderin spots on gradient echo T2*-weighted magnetic resonance imaging are associated with past history of small vessel disease in patients with intracerebral hemorrhage. *J Neuroimaging* 2004; **14:** 251–57.

45 Fan YH, Mok VC, Lam WW, Hui AC, Wong KS. Cerebral microbleeds and white matter changes in patients hospitalized with lacunar infarcts. *J Neurol* 2004; **251:** 537–41.

46 Wardlaw JM, Lewis SC, Keir SL, Dennis MS, Shenkin S. Cerebral microbleeds are associated with lacunar stroke defined clinically and radiologically, independently of white matter lesions. *Stroke* 2006; **37:** 2633–36.

47 Cordonnier C, van der Flier WM, Sluimer JD, Leys D, Barkhof F, Scheltens P. Prevalence and severity of microbleeds in a memory clinic setting. *Neurology* 2006; **66:** 1356–60.

48 Pettersen JA, Sathiyamoorthy G, Gao F, et al. Microbleed topography, leukoaraiosis, and cognition in probable Alzheimer disease from the Sunnybrook Dementia Study. *Arch Neurol* 2008; **65:** 790–795.

49 Qiu C, Cotch MF, Sigurdsson S, et al. Retinal and cerebral microvascular signs and diabetes: the Age, Gene/Environment Susceptibility-Reykjavik study. *Diabetes* 2008; **57:** 1645–50.

50 Lee SH, Park JM, Kwon SJ, et al. Left ventricular hypertrophy is associated with cerebral microbleeds in hypertensive patients. *Neurology* 2004; **63:** 16–21.

51 Lee SH, Bae HJ, Yoon BW, Kim H, Kim DE, Roh JK. Low concentration of serum total cholesterol is associated with multifocal signal loss lesions on gradient-echo magnetic resonance imaging: analysis of risk factors for multifocal signal loss lesions. *Stroke* 2002; **33:** 2845–49.

52 Amarenco P, Bogousslavsky J, Callahan A, et al. High-dose atorvastatin after stroke or transient ischemic attack. *N Engl J Med* 2006; **355:** 549–59.

53 Goldstein LB, Amarenco P, Szarek M, et al. Hemorrhagic stroke in the Stroke Prevention by Aggressive Reduction in Cholesterol Levels study. *Neurology* 2008; **70:** 2364–70.

54 Greenberg SM, Rebeck GW, Vonsattel JPV, Gomez-Isla T, Hyman BT. Apolipoprotein E e4 and cerebral hemorrhage associated with amyloid angiopathy. *Ann Neurol* 1995; **38:** 254–59.

55 Chalmers K, Wilcock GK, Love S. APOE epsilon 4 influences the pathological phenotype of Alzheimer's disease by favouring cerebrovascular over parenchymal accumulation of A beta protein. *Neuropathol Appl Neurobiol* 2003; **29:** 231–38.

56 Pathological correlates of late-onset dementia in a multicentre, community-based population in England and Wales. Neuropathology Group of the Medical Research Council Cognitive Function and Ageing Study (MRC CFAS). *Lancet* 2001; **357:** 169–75.

57 Bennett DA, Schneider JA, Arvanitakis Z, et al. Neuropathology of older persons without cognitive impairment from two community-based studies. *Neurology* 2006; **66:** 1837–44.

58 Greenberg SM, Eng JA, Ning M, Smith EE, Rosand J. Hemorrhage burden predicts recurrent intracerebral hemorrhage after lobar hemorrhage. *Stroke* 2004; **35:** 1415–20.

59 Soo YO, Yang SR, Lam WW, et al. Risk versus benefit of anti-thrombotic therapy in ischaemic stroke patients with cerebral microbleeds. *J Neurology* (in press).

60 Nighoghossian N, Hermier M, Adeleine P, et al. Old microbleeds are a potential risk factor for cerebral bleeding after ischemic stroke: a gradient-echo T2*-weighted brain MRI study. *Stroke* 2002; **33:** 735–42.

61 Kidwell CS, Saver JL, Villablanca JP, et al. Magnetic resonance imaging detection of microbleeds before thrombolysis: an emerging application. *Stroke* 2002; **33:** 95–98.

62 Fiehler J, Albers GW, Boulanger JM, et al. Bleeding risk analysis in stroke imaging before thrombolysis (BRASIL): pooled analysis of T2*-weighted magnetic resonance imaging data from 570 patients. *Stroke* 2007; **38:** 2738–44.

63 Lee SH, Kang BS, Kim N, Roh JK. Does microbleed predict haemorrhagic transformation after acute atherothrombotic or cardioembolic stroke? *J Neurol Neurosurg Psychiatry* 2008; **79:** 913–16.

64 Eckman MH, Wong LK, Soo YO, et al. Patient-specific decision making for warfarin therapy in nonvalvular atrial fibrillation. How will screening with genetics and imaging help? *Stroke* 2008; **39:** 3308–15.

65 Eckman MH, Rosand J, Knudsen KA, Singer DE, Greenberg SM. Can patients be anticoagulated after intracerebral hemorrhage? A decision analysis. *Stroke* 2003; **34:** 1710–16.

66 Viswanathan A, Rakich SM, Engel C, et al. Antiplatelet use after intracerebral hemorrhage. *Neurology* 2006; **66:** 206–09.

67 Lesnik Oberstein SA, van den Boom R, van Buchem MA, et al. Cerebral microbleeds in CADASIL. *Neurology* 2001; **57:** 1066–70.

68 Viswanathan A, Guichard JP, Gschwendtner A, et al. Blood pressure and haemoglobin A1c are associated with microhaemorrhage in CADASIL: a two-centre cohort study. *Brain* 2006; **129:** 2375–83.

69 Werring DJ, Frazer DW, Coward LJ, et al. Cognitive dysfunction in patients with cerebral microbleeds on T2*-weighted gradient-echo MRI. *Brain* 2004; **127:** 2265–75.

70 Viswanathan A, Godin O, Jouvent E, et al. Impact of MRI markers in subcortical vascular dementia: a multi-modal analysis in CADASIL. *Neurobiol Aging* 2008; published online October 14. DOI:10.1016/j.neurobiolaging.2008.09.001.

71 DeCarli C, Fletcher E, Ramey V, Harvey D, Jagust WJ. Anatomical mapping of white matter hyperintensities (WMH): exploring the relationships among periventricular WMH, deep WMH, and total WMH burden. *Stroke* 2005; **36:** 50–55.